

See discussions, stats, and author profiles for this publication at: <https://www.researchgate.net/publication/231681605>

Surface Chemistry of Acetone on Metal Oxides: IR Observation of Acetone Adsorption and Consequent Surface Reactions on Silica–Alumina versus Silica and Alumina

ARTICLE *in* LANGMUIR · NOVEMBER 1999

Impact Factor: 4.46 · DOI: 10.1021/la990739q

CITATIONS

48

READS

124

4 AUTHORS, INCLUDING:



Mohamed I Zaki

Minia University

188 PUBLICATIONS 3,613 CITATIONS

SEE PROFILE



F. Al-Sagheer

Kuwait University

48 PUBLICATIONS 706 CITATIONS

SEE PROFILE

Surface Chemistry of Acetone on Metal Oxides: IR Observation of Acetone Adsorption and Consequent Surface Reactions on Silica–Alumina versus Silica and Alumina

M. I. Zaki,* M. A. Hasan, F. A. Al-Sagheer, and L. Pasupulety

Chemistry Department, Faculty of Science, Kuwait University,
P.O. Box 5969 Safat, 13060 Kuwait

Received June 9, 1999. In Final Form: September 13, 1999

Pathways and generated surface species of adsorption and consequent surface reactions of acetone vapor on characterized silica, alumina, and ~5 wt % silica–alumina were examined by *in-situ* infrared (IR) spectroscopy, following degassing at room (RT) and higher temperatures (100–400 °C). For reference and confirmatory purposes, adsorptives of mesityl oxide and acetic acid, and adsorbents of K-modified and pyridine-covered silica–alumina, were employed. In the absence of Lewis and Bronsted acid sites, as well as of basic sites (i.e., on silica), acetone molecules are weakly hydrogen-bonded to surface OH^{δ+} groups to desorb completely at 100 °C, without involvement in any further surface reactions. The availability of such acid–base sites on alumina and silica–alumina facilitates acetone chemisorption and activation for aldol condensation type surface reactions, leading to formation of surface species of mesityl oxide at RT to 200 °C and their oxidative conversion into acetate species at 300–400 °C. A more obvious availability of Bronsted acid sites on silica–alumina enhances progression of the surface reactions involved.

Introduction

Catalytic hydrogenation of acetone on metal oxide–supported Ni, Co, and Fe metal particles^{1–5} is a potential synthetic route to fine chemicals, such as 4-hydroxy-4-methylpentan-2-one, methyl isobutyl ketone (MIBK), diacetone alcohol (DAA), and mesityl oxide (MSO). Aldol condensation of acetone has been considered^{1–5} the key surface process in the catalytic synthesis of these industrially and technologically important materials. In the liquid phase,⁶ a base (OH[–]) catalyzes removal of a proton from the ketone to give a carbanion (enolic form), which then adds to the carbonyl double bond, yielding DAA. Further acid-catalyzed dehydration of DAA gives MSO, which is then hydrogenated to give MIBK. In order to comprehend the surface chemistry involved in this catalytic process, a systematic *in-situ* IR investigation of acetone vapor adsorption and surface reactions on metal and metal oxide particles is being carried out in this laboratory. The present paper is devoted, however, to present and discuss results of room temperature (RT) adsorption of acetone on silica–alumina *versus* silica and alumina, and its high-temperature consequences. Adopting these particular adsorbents, the main objective was to probe the influence of the surface acid–base properties. Therefore, the silica–alumina utilized was a low-silica

(~5 wt % SiO₂) Akzo product, which has been reported⁷ to assume surfaces exposing SiAlO_x species and exhibiting an intermediate zero-charge point (pH ~ 4–5)⁸ between those of silica (pH ~ 1–2)⁹ and alumina (pH ~ 7–8).⁹ Pyridine was the IR probe molecule used to characterize the surface acid sites available.^{10–12}

A number of IR studies of acetone adsorption on metal oxide surfaces have been reported in the literature, and a good part of them has been reviewed by Knözinger et al.^{10,13} However, only a few such studies have been published.^{10,13–17} considering adsorbents in the silica–alumina system. Young and Sheppard¹⁴ have examined adsorbed species of acetone, *versus* those of acetaldehyde, on Cab–O–Sil silica at RT to 200 °C and confirmed the irreversible uptake of acetone molecules at RT via hydrogen-bonding (H-bonding) interactions to surface silanol groups (Si–OH). These authors found the adsorbed acetone to desorb near 120 °C without chemical modification, unlike adsorbed acetaldehyde, which was consequently involved in a surface (acid)-catalyzed aldol condensation reaction to yield surface crotonaldehyde species. Okunev et al.¹⁵ have correlated sorption isotherms and IR spectra of acetone/silica gel near RT to discern two differently H-bonded acetone species: (i) an acetone molecule H-bonded simultaneously to two adjacent Si–

* Corresponding author. E-mail: zaki@kucol.kuniv.edu.kw. Fax: (0965)4846946.

(1) Narayanan, S.; Unnikrishnan, R. *Appl. Catal. A* **1996**, *145*, 231.
(2) Narayanan, S.; Unnikrishnan, R. In *Recent Advances in Basic and Applied Aspects of Industrial Catalysis*; Prasada Rao, T. S. R., Dhar, M., Eds.; Studies in Surface Science and Catalysis; Elsevier: Amsterdam, 1998; Vol. 113, pp 799–807.
(3) Narayanan, S.; Unnikrishnan, R. *J. Chem. Soc., Faraday Trans. 1998*, *94*, 1123.
(4) Gandia, L.; Montes, M. *Appl. Catal. A* **1993**, *101*, L1.
(5) Grange, P.; Bastians, Ph.; Conacec, R.; Marchand, R.; Laurent, Y.; Gandia, L.; Montes, M.; Fernández Sanz, J.; Odriozola, J. A. *Stud. Surf. Sci. Catal.* **1995**, *91*, 381.
(6) Mackie, R. K.; Smith, D. M.; Alan Aitken, R. *Guidebook to Organic Synthesis*, 2nd ed.; Longman Group Ltd.: Essex, U.K., 1996; pp 86–87.

(7) Espie, A. W.; Vickerman, J. C. *J. Chem. Soc., Faraday Trans. 1* **1984**, *80*, 1903.
(8) Jordan, A.; Kappenstein, C.; Colnay, E.; Zaki, M. I. *J. Chem. Soc., Faraday Trans. 1998*, *94*, 1156.
(9) Parks, G. A. *Chem. Rev.* **1965**, *65*, 177.
(10) Boehm, H.-P.; Knözinger, H. In *Catalysis—Science and Engineering*; Anderson, J. R., Boudart, M., Eds.; Springer-Verlag: Berlin, 1983; Vol. 4, pp 39–207.
(11) Paukshtis, E. A.; Yurchenko, E. N. *Russ. Chem. Rev.* **1983**, *52*, 242.
(12) Ferwerda, R.; van der Mass, J. H.; van Duijneveldt, F. B. *J. Mol. Catal. A* **1996**, *104*, 319.
(13) Ertl, G.; Knözinger, H.; Weitkamp, J., Eds. *Handbook of Heterogeneous Catalysis*; Wiley-VCH: Weinheim, 1997; Vol. 5.
(14) Young, R. P.; Sheppard, N. *J. Catal.* **1967**, *7*, 223.
(15) Okunev, A. G.; Paukshtis, E. A.; Aristov, Y. I. *React. Kinet. Catal. Lett.* **1998**, *65*, 161.

OH groups (strong bonding) and (ii) an acetone molecule H-bonded to a single isolated Si–OH (weak bonding). Allian et al.¹⁶ have examined adsorption of a series of carbonyl compounds (C₁–C₆) on intensively dehydroxylated Degussa Aerosil silica, in order to determine the magnitudes of the thermodynamic functions of the adsorptive interactions involved. Acetone has been thereby found¹⁶ to adsorb not only via H-bonding to isolated Si–OH groups at RT but also via a contribution of van der Waals type interactions. Panov and Fripiat¹⁷ have investigated low-temperature (\leq RT) adsorption of acetone and MSO on a series of variously composed (Si/Al) zeolitic materials. Those authors have communicated IR evidence for the involvement of adsorbed acetone in the aldol condensation reaction to give MSO surface species at RT, which is in concord with what has been observed on some transition metal oxides.^{18,19} Thus, the importance of the availability of surface Lewis (L) acid sites for acetone condensation has been highlighted. However, those authors have not probed the mechanistic pathways of the surface reactions involved, the role of Bronsted (B) acid sites in the course of the reaction, and the impacts of high-temperature ($>$ RT) regimes.

Therefore, the present investigation employs *in-situ* IR spectroscopy to examine RT adsorption of acetone vapor on modified and unmodified surfaces of \sim 5 wt % silica–alumina and effects of subsequent high-temperature degassing (at 100–400 °C) on the stability and chemical composition of the adsorbed species. For reference purposes, the same was applied using unmodified silica and alumina as adsorbents. Besides, IR spectra were taken of RT and high-temperature adsorbed species of vapors of MSO and acetic acid. The modification of silica–alumina was confined to the surface and was effected by (i) impregnation with potassium ions and (ii) monolayer coverage with pyridine molecules. The bulk and surface properties of the adsorbents were characterized by X-ray powder diffractometry and photoelectron spectroscopy, IR spectroscopy of adsorbed pyridine, and BET analysis of nitrogen adsorption isotherms at liquid nitrogen temperature.

Experimental Section

Adsorbents. Unmodified adsorbents were Degussa Aluminomox C (denoted Al) and Aerosil-200 (Si) and Akzo 5 wt % silica–alumina (SiAl). Modified SiAl samples were obtained either by impregnation with an aqueous solution (15 mL/g of SiAl) of KNO₃, to load 6 wt % K,⁸ or by coverage with irreversibly held pyridine (Py) molecules at RT. Both materials are denoted, respectively, by K-SiAl and Py-SiAl. Samples of the unmodified and K-modified adsorbents were *ex-situ* calcined at 400 °C for 2 h, in order to obtain similar samples to those pretreated *in-situ* (*vide infra*).

Adsorptives. The vapor phases in equilibrium with deaerated portions of AR-grade liquid acetone (Ac), mesityl oxide (MSO), acetic acid (AcAc), and pyridine (Py) at RT were the adsorptives applied. The liquids were products of BDH/U.K. and were deaerated by on-line freeze–pump–thaw cycles performed at liquid nitrogen temperature.

Characterization of Adsorbents. The bulk crystalline structure of the adsorbents was determined by X-ray powder diffractometry (XRD). Moreover, the surface area was determined by BET analysis of N₂ adsorption isotherms, the chemical composition by X-ray photoelectron spectroscopy (XPS), the functional atomic groups by *in-situ* IR spectroscopy (*vide infra*),

and the acid sites by *in situ* IR spectroscopy of adsorbed Py at RT (*vide infra*).

XRD was carried out (at $2\theta = 10$ – 80° and RT) using a model D5000 Siemens diffractometer (Germany) equipped with Ni-filtered Cu K α radiation ($\lambda = 1.5406$ Å). The diffractometer was operated with 1° diverging and receiving slits at 50 kV and 40 mA, and a continuous scan was carried out with a step size of 0.04° and a step time of 2 s. An on-line automatic search system (PDF Data Base) facilitated an observed data match with JCPDS standards. Particle sizing was realized adopting the line-broadening technique and Sherrer formula.²⁰

N₂ adsorption isotherms were determined on adsorbents at liquid nitrogen temperature (-195°C), using an automatic ASAP 2010 Micromeritics sorpometer (U.S.A.) equipped with a degassing platform and an on-line data acquisition and handling system loaded with BET-based²¹ analytical software for the surface area (m²/g of adsorbent) determination. The N₂ gas was a 99.999% pure product of KOAC (Kuwait), and the adsorbents (500 ± 2 mg) were pre-degassed at 110°C and 10^{-5} Torr (1 Torr = 133.3 Pa) for 3 h.

XPS spectra were recorded on a model VG Scientific 200 (U.K.) spectrometer using Al K α radiation (1486.6 eV) operating at 300 W, 13 kV, and 23 mA. The spectra acquisition and handling were carried out by means of an on-line Eclipse data system (U.K.). The test materials were compacted onto the sample holder (8 mm in diameter) in an ambient atmosphere, mounted and stored in the introduction chamber until a vacuum of 10^{-9} to 10^{-10} Torr was reached, and, then, transferred into the analysis chamber for data acquisition (0.2 eV step; 250 ms dwell time; 0.7 eV resolution; up to 10 scans). All binding energy values were determined with respect to the C(1s) line (284.6 eV) originating from adventitious carbon, and the standard deviation of the peak position was estimated to be ± 0.02 eV. The surface atomic percentage (%) of the elements observed was calculated from the peak areas (in counts eV/s) with integral subtraction of the background.

***In-Situ* IR Spectroscopy of Adsorbed Species.** Thin, but intact, self-supporting wafers (30 ± 5 mg/cm²) of test adsorbents were prepared (under 0.5 ton/cm²) and mounted inside a specially designed, heatable, and evacuable all-Pyrex glass IR cell similar to that designed by Peri.²² The cell, equipped with CaF₂, was hooked to an all-Pyrex glass Gas/Vac handling system and briefly evacuated at RT. Then, a stream (50 cm³/min) of 99.9% pure O₂ (KOAC) was allowed throughout the cell. The wafer was heated in the O₂ atmosphere at 400°C for 30 min and then cooled to 300°C , prior to subjection to degassing for 60 min at 10^{-6} Torr. Subsequently, the wafer was cooled under dynamic vacuum to RT, and cell and adsorbent IR background spectra were taken (average of accumulated 100 scans) over the frequency range 4000 – 400 cm⁻¹ and at a resolution of 4.0 cm⁻¹ and room (beam) temperature, using a model SPECTRUM-BX FTIR Perkin-Elmer (Germany) spectrometer. The sample compartment was purged with dry N₂ for 10 min prior to recording the spectra. A difference spectrum (adsorbent *minus* cell background spectrum) obtained using the installed spectra acquisition and handling system, P-E Spectrum v2.0 software, provided the basis for determination of the surface functional groups (*vide supra*). The cell was rehooked to the Gas/Vac line, and a 10 -Torr portion of Ac vapor (or 2 – 3 Torr of MSO, AcAc, or Py) was expanded into it at RT. A spectrum of the gas phase (gas phase *plus* cell background) was recorded, prior to a 5-min degassing of the cell (at RT) and taking a spectrum of the adsorbent *plus* adsorbed species (*plus* cell background). By subtraction of the cell and adsorbent background spectra, IR difference spectra of the gas phase and adsorbed species were respectively obtained. Then, the wafer (*plus* adsorbed species) was degassed while being heated to 100°C and was cooled under vacuum to RT, and a spectrum was recorded of the wafer (*plus* residual adsorbed species). The same process was followed for 200 , 300 , and 400°C .

(20) Matyi, R. J.; Schwartz, L. H.; Butt, J. B. *Catal. Rev.—Sci. Eng.* **1987**, *29*, 41.

(21) Lecloux, A. J. In *Catalysis—Science and Technology*; Anderson, J. R., Boudart, M., Eds.; Springer-Verlag: Berlin, 1981; Vol. 2, pp 171–229.

(22) Peri, J. B.; Hannan, R. B. *J. Phys. Chem.* **1960**, *64*, 1526.

(23) Kline, C. H., Jr.; Turkevich, J. *J. Chem. Phys.* **1944**, *12*, 300.

(16) Allian, M.; Borello, E.; Ugliengo, P.; Spanò, G.; Garrone, E. *Langmuir* **1995**, *11*, 4811.

(17) Panov, A.; Fripiat, J. J. *Langmuir* **1998**, *14*, 3788.

(18) Miyata, H.; Toda, Y.; Kubokawa, Y. *J. Catal.* **1974**, *32*, 155.

(19) Busca, G.; Lorenzelli, V. *J. Chem. Soc., Faraday Trans. 1* **1982**, *78*, 2911.

Table 1. Bulk and Surface Characteristics of the Adsorbents

adsorbent	bulk		surface			
	crystalline phase composition	JCPDS card no.	BET-area/ m ² g ⁻¹	chemical composition ^a	functional groups ^a	acid sites ^{a,b}
SiAl ^c	microcrystalline SiO ₂ , <i>m</i> (4.1 nm) ^f γ -Al ₂ O ₃ , <i>j</i> (3.7 nm)	12-0708 29-0063	383 (387) ^d	O ²⁻ (+ OH and H ₂ O, 50.4%) ^e Al ³⁺ (49.5%) Si ⁴⁺ ($\leq 0.1\%$)	Al-OH; (Al) ₂ OH; (Al) ₃ OH; AlOSi(?); CH _x (ip); ^g CO _x (ip)	HB-donor H ⁺ -donor cu-Al ³⁺
Si	none		182 (198)	O ²⁻ (+ OH and H ₂ O, 62.6%) Si ⁴⁺ (37.4%)	isolated Si-OH; (Si) ₂ OH; (Si) ₂ O; CH _x (ip)	HB-donor
Al	microcrystalline γ -Al ₂ O ₃ , <i>j</i> (14 nm) δ -Al ₂ O ₃ , <i>m</i> (6 nm)	29-0063 04-0877	111 (107)	O ²⁻ (+ OH and H ₂ O, 60.4%) Al ³⁺ (39.6%)	Al-OH; (Al) ₂ OH; (Al) ₃ OH; CH _x (ip); CO _x (ip)	HB-donor H ⁺ -donor cu-Al ³⁺

^a Measurements were carried out following *in-situ* treatments of adsorbents in O₂ at 400 °C and degassing at 300 °C. ^b Proton (H⁺) donor sites were more obvious on SiAl than Al. ^c Examination of K-SiAl has characterized rather similar bulk and surface properties, except for the following: (i) surface chemical composition [O²⁻ (56.5%), Al³⁺ (38.4%), K⁺ (4.8%), and Si⁴⁺ (0.3%); (ii) functional groups [acidic Al-OH and (Al)₂OH groups were largely converted into Al-OK groups].⁸ ^d Parenthesized value is for corresponding 400 °C calcination product. ^e Numerical value is for surface atomic percentage of corresponding species. ^f Parenthesized value is for the average crystallite size, as determined from XRD line broadening.²⁰ ^g ip = impurity; HB = hydrogen bond; cu = coordinatively unsaturated.

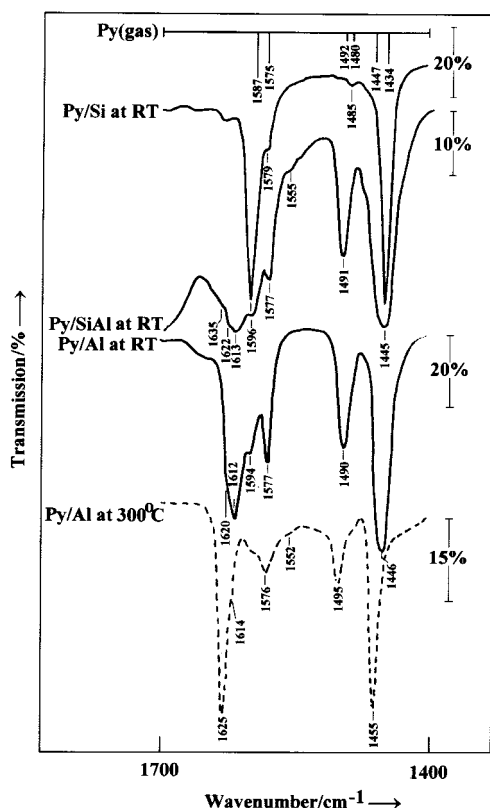


Figure 1. IR ν CCN spectra of pyridine (Py)-adsorbed species established on the adsorbents indicated at RT. The spectra of the 300 °C Py-adsorbed species on Al, and the indicated frequency values and relative intensities of ν CCN vibrations of gas-phase Py (see top), are inset for comparison purposes.

Results and Discussion

Characteristics of Adsorbents. Table 1 indicates that Si is noncrystalline and has high-area surfaces (182 m²/g) composed chemically of Si⁴⁺, O²⁻, and OH groups. The XPS-determined O/Si atomic ratio (~ 1.7) is slightly short of that demanded by the composition SiO₂. *In-situ* IR analysis of the material revealed the presence of the following surface groups: isolated Si-OH and (Si)₂OH, (Si)₂O, associated (H-bonded) OH's, as well as a small proportion of CH_x impurity species. The IR ν CCN spectrum taken from Py/Si at RT (Figure 1) displays absorption bands at 1596, 1579, 1485, and 1445 cm⁻¹. According to the reference data compiled in Table 2, these bands are indicative of HPy species (=H-bonded Py molecules). Consistently, IR ν OH absorption of Si-OH groups (3744

Table 2. ν CCN Vibration Modes and IR Absorption Frequencies of Gas-Phase, Liquid-Phase, and Adsorbed Pyridine (Py)

ν CCN modes ^a	frequency/cm ⁻¹				
	gas ^b	liquid ^c	HPy ^{d,e}	LPy ^{d,e}	BPy ^{d,e}
19b	1434	1438	1440–1445	1445–1460	1530–1550
19a	1447	1482	1480–1490	1478–1490	1470–1490
8b	1575	1582	1577–1580	1575–1585	1600–1613
8a	1587	1598	1580–1600	1602–1632	1631–1640

^a Modes as assigned in refs 12 and 23. ^b Present investigation. ^c Data adopted from ref 24. ^d Data abstracted from refs 11 and 25. ^e HPy = H-bonded Py; LPy = Py coordinated to Lewis acid (cu) sites; BPy = Py bound to Brønsted acid (H⁺-donor) sites.

cm⁻¹) has been largely suppressed and a broad absorption due to associated OH groups (centered around 3440 cm⁻¹) has concomitantly been intensified. As expected,¹⁰ the ν CCN bands have been eliminated, and the changes conceded by the ν OH spectrum have been lifted, upon degassing of Py/Si at 100 °C. These results indicate that surfaces of Si only expose H-bond donor sites associated mainly with isolated OH groups (Table 1).

Table 1 shows the bulk structure of Al to be constituted of microcrystallites of γ -Al₂O₃ (major) and δ -Al₂O₃ (minor). The surface is shown to assume an area of 111 m²/g and a chemical composition made up of Al³⁺, O²⁻, OH, and H₂O with a O/Al atomic ratio (~ 1.52) almost identical to that demanded by the Al₂O₃ composition. The surface functional groups detected include various types of hydroxyl groups [terminal, Al-OH; bridging, (Al)₂OH; and multicentered, (Al)₃OH],¹⁰ as well as small proportions of CH_x and CO_x impurity species. The IR ν CCN spectrum taken from Py/Al at RT (Figure 1) probes HPy species (absorptions at 1594, 1577, and 1446 cm⁻¹) similar to those observed in Py/Si and displays additional absorptions at 1620(sh), 1612, and 1490 cm⁻¹. Upon degassing at 100 °C, HPy species were partially eliminated, but complete elimination was not accomplished until 200 °C. Simultaneously, the absorption at 1612 cm⁻¹ was markedly weakened, whereas those at 1620, 1577, 1490, and 1446 cm⁻¹ persisted, getting slightly weaker and slimmer, and suffered slight frequency shifts. Figure 1 shows, moreover, that these persistent absorptions also remained stable to degassing at 300 °C; they were not eliminated until the temperature of 400 °C was reached (weak bands due to α -pyridone conversion species were observed).¹⁰ These results are consistent with previous studies¹⁰ and data given in Table 2, in showing Py/Al to include not only HPy but also different LPy species (Py coordinated to two different types of Lewis acid sites: weak L-sites, monitored by the ν CCN absorption at 1612 cm⁻¹, and strong L-sites,

characterized by the absorption at 1625 cm^{-1} .¹⁰ It is worth noting, however, that the very weak shoulder at 1552 cm^{-1} might be originating from a minute proportion of BPy species (protonated Py, Table 2). Thus, Table 1 suggests the exposure on Al of an H-bond donor (associated with $\text{OH}^{\delta+}$ groups) and two different L-sites (associated with cu-Al^{3+} sites of different states of coordination unsaturation (cu)),¹⁰ and presumes availability of some Bronsted (B) acid sites (associated with OH^+ and/or coordinated H_2O molecules).¹⁰

SiAl is shown (Table 1) to assume a bulk structure consisting of microcrystallites of $\gamma\text{-Al}_2\text{O}_3$ (major) and SiO_2 (minor), and a surface area of $383\text{ m}^2/\text{g}$. The surface chemical composition appears to consist of O^{2-} , Al^{3+} , OH , H_2O , and a minute proportion of Si^{4+} . The detection of only a minority proportion of surface Si^{4+} contradicts the results of an earlier study,⁷ which has revealed a similar 5 wt % silica–alumina material to expose silica-dominated surfaces. A plausible explanation may be based on the heat-assisted crystallization of the SiO_x component of the present adsorbent into XRD-detectable SiO_2 microcrystallites (Table 1). The fact that the surface atomic ratio of oxygen to the total metal sites (1.02%) is almost unity may assume that the surface composition of SiAl is not intimately related to the bulk crystalline structure. The surface functional groups probed are associated mainly with the AlO_x component, with a possible formation of Al-O-Si bridges (Table 1). However, the existence of Si-OH groups (νOH at 3744 cm^{-1}) cannot be excluded with certainty. The IR νCCN spectrum taken from Py/SiAl at RT (Figure 1) probes formation of HPy (band at 1596 cm^{-1}), LPy (bands at 1613 and 1622 cm^{-1}), and BPy (absorptions at 1555 and 1635 cm^{-1}) species (Table 2). Thus, SiAl surfaces are similar to those of Al in exposing $\text{OH}^{\delta+}$ and cu-Al^{3+} sites (Table 1) but are distinct in exhibiting clear indications of the presence of OH^+ sites.

It is worth mentioning that the fact that *ex-situ* calcination of the adsorbents has caused insignificant changes to the surface area (Table 1) may imply that the analogous *in-situ* calcination would do likewise. Table 1 reveals, moreover, that K-modification of SiAl also caused insignificant changes to the bulk and surface properties of SiAl, except for the surface chemical composition and functional groups. The former property has been modified by (i) the exposure of approximately 5 atomic % K, (ii) an enhanced exposure of Si^{4+} sites (from 0.1 to 0.3%), and (iii) an increased O to (total) metal atomic ratio from 1 to 1.3. On the other hand, the latter property has been modified by a considerable conversion of surface-OH groups into surface-OK groups, mainly involving the acidic ones (bridging and multicentered).

IR Spectra of Adsorptives. Figure 2 compares IR gas-phase spectra taken from 10 Torr of Ac and 3 Torr of MSO at room (beam) temperature over the $\nu\text{CO}/\delta\text{CH}$ frequency range ($1800\text{--}1300\text{ cm}^{-1}$). Assignments and frequencies of absorptions displayed in this range, as well as of those displayed at $1300\text{--}1000\text{ cm}^{-1}$, are summarized in Table 3. The table sets out frequencies of similar absorptions monitored in the liquid-phase spectra of both Ac and MSO.²⁴ Figure 2 reveals that the most prominent differences between the IR characteristics of gas-phase

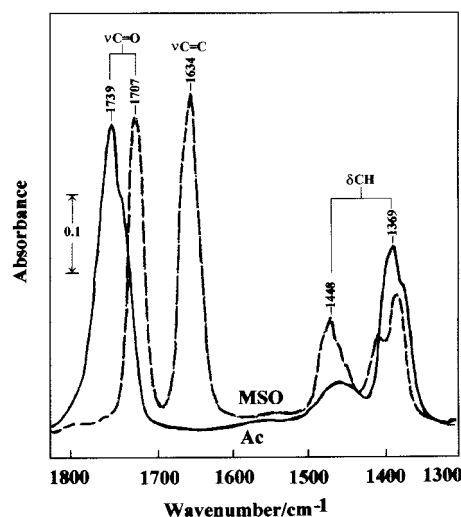


Figure 2. IR $\nu\text{C=O}/\delta\text{CH}$ spectra of 10 Torr of gas-phase acetone (Ac) and 3 Torr of gas-phase mesityl oxide (MSO) at RT.

Table 3. Assignments and Frequencies of IR Absorptions (at $1800\text{--}950\text{ cm}^{-1}$) of Acetone (Ac) and Mesityl Oxide (MSO) in the Gas and Liquid Phases

assignment ^a	Ac		MSO	
	gas/ cm^{-1} ^b	liquid/ cm^{-1} ^c	gas/ cm^{-1} ^b	liquid/ cm^{-1} ^d
$\nu\text{C=O}$	1738 (vs) ^e	1716 (vs)	1707 (vs)	1690 (vs)
$\nu\text{C=C}$			1634 (vs)	1620 (vs)
δCH	1436 (m)	1420 (m)	1448 (m)	1449 (m)
	1367 (vs)	1364 (vs)	1389 (m)	1379 (m)
	1352 (sh,vs)		1365 (m)	1358 (m)
$\nu\text{C-C}$	1225 (vs)	1288 (vw)	1294 (vs)	1220 (s)
	1215 (vs)	1222 (vs)		
	1201 (sh,vs)	1183 (vw)	1187 (w)	1183 (w)
$(\text{CH}_3)_r^f$	1092 (w)	1094 (w)	1065 (vw)	965 (w)

^a As given in refs 17 and 26. ^b Present work. ^c In ref 24, p 91. ^d In ref 24, p 356. ^e s, strong; vs, very strong; m, medium; sh, shoulder; w, weak; vw, very weak. ^f $(\text{CH}_3)_r$ = methyl rocking.

Ac and MSO are the $\nu\text{C=C}$ and δCH absorptions displayed in the spectrum of MSO at 1634 and 1448 cm^{-1} , respectively. The comparison held in Table 3 may help with realizing the impacts of intermolecular (physical) interactions occurring in each material (Ac or MSO), which maximize in the liquid phase, on the IR characteristics. It is obvious that these intermolecular interactions cause detectable low-frequency shifts to most vibrations of the functional groups involved, particularly to those of $\nu\text{C=O}$ and $\nu\text{C=C}$. Similar interactions are expected to prevail in closely packed physisorbed layers.

Room-Temperature Adsorption of Acetone Vapor.

Figure 3 compares IR $\nu\text{OH}/\nu\text{CH}$ and $\nu\text{CO}/\delta\text{CH}/\nu\text{CC}$ spectra of adsorbed species following RT adsorption of Ac on Si, Al, and SiAl with those shown by Ac molecules in the gas phase. The spectrum taken from Ac/Si monitors strong twin bands at 1708 and 1699 cm^{-1} and two weak bands at 1605 and 1425 cm^{-1} , as well as a medium band at 1327 cm^{-1} . According to the reference data compiled in Table 4, these bands can account for H-bonded Ac molecules. Okunev et al.¹⁵ have come across similar results for Ac adsorbed on hydroxylated silica gel and assigned $\nu\text{C=O}$ bands at 1705 and 1690 cm^{-1} to Ac molecules H-bonded to single and pair sites of Si-OH groups, respectively. Consistently, the spectrum (Figure 3) shows νOH absorption of isolated Si-OH groups to suffer a considerable low-frequency shift ($3743 \rightarrow 3454\text{ cm}^{-1}$) following acetone adsorption.

(24) Pachler, K. G. R.; Matlok, F.; Gremlich, H.-U., Eds. *Merck FT-IR Atlas*; VCH: Weinheim, 1988; p 214.

(25) Connell, G.; Dumeric, J. A. *J. Catal.* **1986**, *101*, 103.

(26) Dellepiane, G.; Overend, J. *Spectrochim. Acta* **1966**, *22*, 593.

(27) Kubelková, L.; Čejka, J.; Nováková, J. *Zeolites* **1991**, *11*, 48.

(28) McManus, J. C.; Harano, Y.; Low, M. J. *Can. J. Chem.* **1969**, *47*, 2545.

(29) Gruver, V.; Panov, A.; Fripiat, J. J. *Langmuir* **1996**, *12*, 2505.

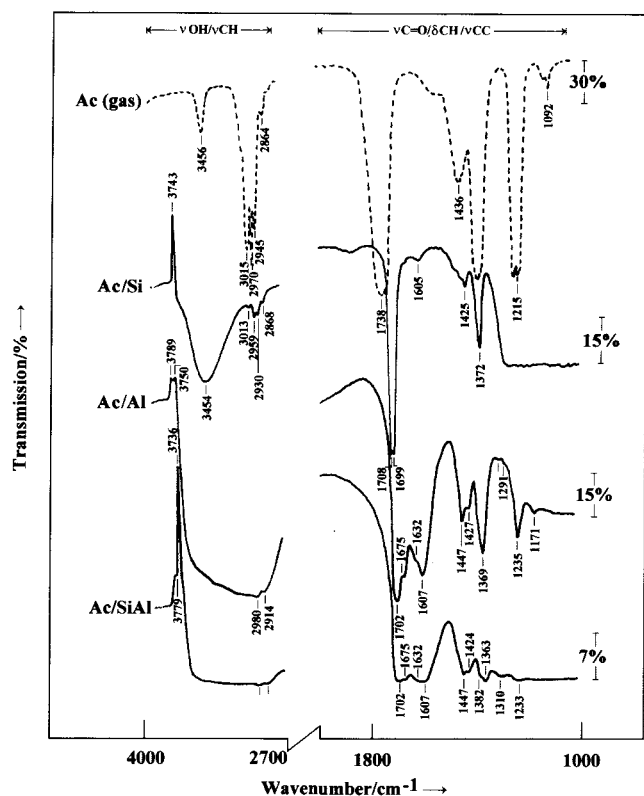


Figure 3. IR $\nu\text{OH}/\nu\text{CH}$ and $\nu\text{C}=\text{O}/\delta\text{CH}/\nu\text{CC}$ spectra taken from adsorbed species following exposure of the indicated adsorbents to acetone vapor and degassing at RT. The spectra of gas-phase acetone (---) are inset for comparison purposes.

Spectra monitoring IR characteristics of Ac adsorbed species on Al and SiAl at RT (Figure 3) display two largely similar sets of absorptions at 1800–1000 cm^{-1} , though with different intensities. They also show considerable low-frequency shifts of νOH absorptions of surface OH groups. According to Boehm and Knözinger,¹⁰ the OH's involved (Al, νOH at 3789 and 3750 cm^{-1} ; SiAl, νOH at 3779 and 3736 cm^{-1}) are terminal and bridging Al–OH groups on both adsorbents. In terms of the data compiled in Table 4, the absorptions of adsorbed Ac are indicative of acetone molecules coordinated to cu-Al^{3+} sites ($\nu\text{C}=\text{O}$ at 1702 and 1675 cm^{-1}), MSO coordinated to cu-Al^{3+} sites ($\nu\text{C}=\text{O}$ at 1675 cm^{-1} and $\nu\text{C}=\text{C}$ at 1607 cm^{-1}), and most probably H-bonded MSO ($\nu\text{C}=\text{O}$ at 1632 cm^{-1}).

For confirmatory purposes, a spectrum taken from adsorbed species established following exposure of Al to MSO vapor and subsequent degassing at RT is displayed in Figure 4. The spectrum can aid in recognizing absorptions due to adsorbed MSO in the spectra of Ac/Al and Ac/SiAl at ≤ 1447 cm^{-1} (Figure 3). MSO/Al shows, moreover, strong absorptions at 1616 and 1569 cm^{-1} , which are assignable to protonated MSO species (Table 4). The absence of similar absorption bands in the spectra taken of Ac/Al and Ac/SiAl (Figure 3) may indeed relate the $\nu\text{C}=\text{O}$ absorption at 1632 cm^{-1} to H-bonded MSO rather than to protonated MSO. It is the formation of such species that is most likely responsible for the low-frequency shifts of $\nu\text{AlO}-\text{H}$ absorptions (Figure 3). Following degassing of MSO/Al at 100 $^{\circ}\text{C}$, irreversibly held surface species gave rise to almost the same set of MSO characteristic absorptions at 1681–1569 and ≤ 1447 cm^{-1} , in addition to new absorptions at 1543 and 1470 cm^{-1} . Table 4 may consider the absorption at 1543 cm^{-1} to imply generation of enolate species, whereas a similar absorption to that at 1470 cm^{-1} has been related by Panov and Fripiat¹⁶ to

aromatic condensation species. The present authors prefer to assign the two absorptions to νCOO vibrations of acetate species produced at the expense of MSO surface species. The obvious suppression of the absorption at 1681 cm^{-1} at 100 $^{\circ}\text{C}$ (Figure 4) may imply that coordinated MSO species are mainly those involved in the formation reaction of surface acetates.

The IR spectrum taken from Ac/Py–SiAl at RT (not shown) displayed, in addition to the νCCN absorptions of LPy species (Table 2), weak absorptions (at 1710, 1608, 1430, and 1475 cm^{-1}) assignable to H-bonded Ac molecules (Table 4 and Figure 3 for Py/Si). No sign of formation of MSO surface species was detectable. The absorptions related to adsorbed Ac were almost completely eliminated on degassing at 100 $^{\circ}\text{C}$, thus sustaining their connection to H-bonded Ac. These results may imply that coordinated Ac molecules are precursors for the formation of MSO surface species. This statement was strongly supported by the IR spectrum taken from Ac/K–SiAl (also not shown), which displayed no sign of formation of H-bonded or protonated Ac or MSO, although it monitored $\nu\text{C}=\text{O}$ absorptions (at 1705, 1682, and 1690 cm^{-1}) assignable to coordinated Ac and MSO (Table 4 and Figure 3).

The above results, which are further summarized in Table 5, indicate that adsorbed Ac is partially converted into MSO upon RT adsorption on Al and SiAl, in line with others' findings.^{15,19} The fact that such a conversion is possible neither on Si nor on Py–SiAl may underline the importance of Lewis sites for the necessary activation. In contrast, the occurrence of Ac \rightarrow MSO conversion on K–SiAl may exclude participation of acidic OH's in the surface reaction involved.

High-Temperature Degassing. Figure 4 compares IR $\nu\text{CO}/\delta\text{CH}/\nu\text{CC}$ spectra, revealing impacts of high-temperature degassing (at 100–400 $^{\circ}\text{C}$) on RT-adsorbed Ac on Al and SiAl. A spectrum taken of Ac/Al, following degassing at RT (not shown), declared persistence of coordinated Ac, with conversion of only a small proportion into MSO species. Figure 4 shows that when degassing was carried out at 200 $^{\circ}\text{C}$, Ac/Al exhibited a spectrum comparable to that exhibited by MSO/Al following degassing at 100 $^{\circ}\text{C}$, that is dominated by absorptions assignable to MSO surface species. Similar results are communicated in the spectrum shown by Ac/SiAl following degassing at 100 $^{\circ}\text{C}$ (Figure 4). At 200 $^{\circ}\text{C}$, degassing of Ac/SiAl led to a considerable weakening of IR absorptions of MSO species, with the emergence of two unique absorptions at 1570 and 1470 cm^{-1} . Hence, SiAl surfaces are shown to facilitate Ac conversion reactions, more than Al surfaces do. Following degassing at 300–400 $^{\circ}\text{C}$, both Ac/Al and Ac/SiAl gave rise to spectra similarly dominated by two strong absorptions at 1570–1575 and 1470–1465 cm^{-1} (Figure 4). A similar two absorptions have been frequently encountered in IR studies of high-temperature surface reactions of organic oxygenates^{30,31} and assigned respectively to antisymmetric and symmetric νCOO vibrations of bridging acetate surface species. For confirmatory purposes, adsorbed acetic acid (AcAc) species on Al were subjected to degassing at 400 $^{\circ}\text{C}$, and the resulting IR spectrum, which mainly displays absorptions due to surface acetate groups, is inset in Figure 4.

The above results, which are also summarized in Table 5, indicate that heating activates adsorbed Ac (mainly the coordinated species) for complete conversion into MSO

(30) Hussein, G. A.; Sheppard, N.; Zaki, M. I.; Fahim, R. B. *J. Chem. Soc., Faraday Trans.* **1991**, *87*, 2661.

(31) Zaki, M. I.; Hussein, G. A.; El-Ammawy, H. A.; Mansour, S. A. A.; Poltz, J.; Knözinger, H. *J. Mol. Catal.* **1990**, *57*, 367.

Table 4. Assignments and IR Frequencies of $\nu\text{C}=\text{O}$ and $\nu\text{C}=\text{C}$ of RT Adsorbed Acetone (Ac) and Mesityl Oxide (MSO), as Well as Enolate^a Species, in Various Acid Environments^b

assignment	lit. data			present data	
	Ac ν/cm^{-1}	MSO ν/cm^{-1}	source refs	Ac ν/cm^{-1}	MSO ν/cm^{-1}
C=O, physisorbed	1714–1720	1680–1720	17, 27		1681–1725 ^c
	1690–1715		19		
C=O→L-site	1678–1702	1650–1670	17, 19	1702 and 1675(?)	1675–1681 ^d
	1608–1700		18		
C=O... ⁺ HO-site	1652–1655	1617–1632	17, 27		1616–1632 ^c
C=O... ⁺ HO-site	1682–1715	1630–1635	14–17, 27–29	1699 and 1708	1632 ^d
C=C→L-site		1590–1604	17, 19		1607 ^d
C=C... ⁺ HO-site		1555–1565	17, 19		1569 (?) ^c
C=C... ⁺ HO-site		1570–1594	17, 19		1569 (?) ^c

^a Enolate: lit. data, $\nu\text{C}=\text{C}=\text{O}^-$ at $1540\text{--}1550\text{ cm}^{-1}$; ^{18,19} present work, an absorption appearing at $1543\text{--}1550\text{ cm}^{-1}$ may be due to enolate and/or acetate species. ^b Reported adsorbents: zeolites, HM, ZSM-5a, HY, USY, HZMS-5; ¹⁷ NiO and MgO; ¹⁸ $\alpha\text{-Fe}_2\text{O}_3$; ¹⁹ hydroxylated silica; ^{14,15} largely dehydroxylated silica. ¹⁶ ^c Respective absorption bands dominate at high MSO coverage, that is following exposure to 3 Torr of MSO vapor at RT and brief degassing at the same temperature. ^d Respective absorption bands are observable at low MSO coverage, that is when adsorbed MSO is generated at the expense of adsorbed Ac.

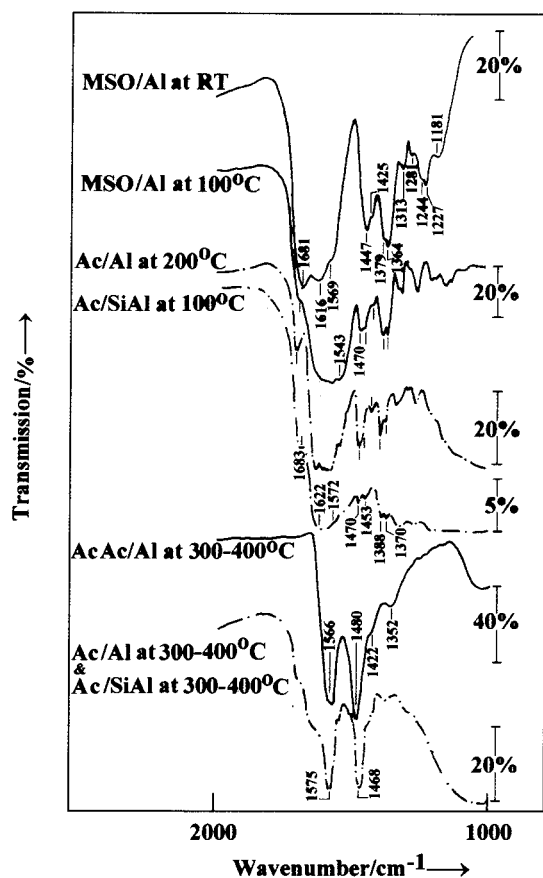


Figure 4. IR $\nu\text{C}=\text{O}/\delta\text{CH}/\nu\text{CC}$ spectra revealing impacts of high-temperature degassing on RT-adsorbed acetone (Ac) on alumina (Al) and silica–alumina (SiAl) as a function of temperature ($100\text{--}400\text{ }^\circ\text{C}$). Spectra taken of adsorbed mesityl oxide (MSO) on Al at RT, and following degassing at $100\text{ }^\circ\text{C}$, are inset for confirmatory purposes.

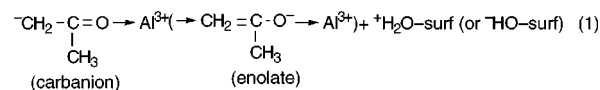
surface species at $100\text{--}200\text{ }^\circ\text{C}$. At higher temperatures ($\geq 200\text{ }^\circ\text{C}$), the MSO species thus generated are activated for conversion into surface acetate species. Busca and Lorenzelli¹⁹ have encountered a similar conversion sequence while examining acetone adsorption on $\alpha\text{-Fe}_2\text{O}_3$. However, these authors have suggested conversion of adsorbed Ac into enolate species, prior to conversion into MSO species. Panov and Fripiat¹⁷ have not come across enough IR evidence to support the suggestion of Busca and Lorenzelli,¹⁹ while looking into acetone adsorption on zeolitic surfaces. However, they agree with them, in proposing an aldol-condensation⁶ type of surface reaction

to undertake the $\text{Ac} \rightarrow \text{MSO}$ conversion *via* formation of enolate and diacetone alcohol (DAA) intermediate species.

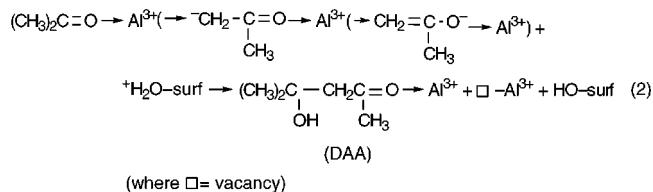
Surface Reactions and Reactivity. The surface reactions discussed in the present section are those responsible for formation and subsequent conversion of MSO into acetate adsorbed species in the course of adsorption of acetone molecules on Al and SiAl. According to various reports^{17–19} formation of MSO from adsorbed Ac occurs most likely *via* an aldol-condensation type of reaction pathway.⁶

In the liquid phase,⁶ aldol (self) condensation of acetone (Ac) molecules involves, as an initial step, base-catalyzed keto \rightarrow enol conversion. In the presence of an acid (Lewis or Bronsted type), an addition reaction of coordinated (or protonated) Ac to the enol form (carbanion) results in the formation of DAA, which is then dehydrated, with the help of Bronsted acid sites, to yield MSO. Thus, the following surface aldol-condensation pathways may be suggested:

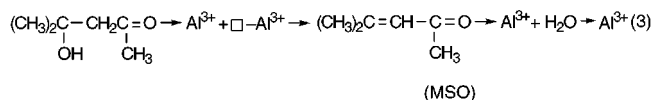
[1] keto \rightarrow enol conversion:



[2] addition reaction:



[3] dehydration reaction:



The inability of Si surfaces to chemisorb and activate Ac molecules for further surface reactions stresses the necessity for available acid–base sites on reactive surfaces. The fact that enolate species were not detectable on the present surfaces, as well as on the analogous zeolitic surfaces,¹⁷ may imply that the keto \rightarrow enol conversion on these surfaces is slower than the subsequent addition reaction. It is probably the availability on these surfaces of Bronsted acid sites (catalyst of the addition reaction)

Table 5. Adsorbed Species Established Following Acetone Adsorption and Surface Reactions on Pure and Modified Silica-Alumina (SiAl) versus Silica (Si) and Alumina (Al), As a Function of Degassing Temperature (RT to 400 °C)

adsorbent	degassing temp/°C	
	RT	100–400
Si	H-bonded Ac ^a	desorbs completely at 100 °C
Al	coordinated Ac ^b coordinated MSO ^c	persists to 100 °C and converts almost completely into MSO at 200 °C largely stable to 200 °C and converts to acetate species at 300–400 °C
SiAl	H-bonded MSO coordinated Ac ^b coordinated MSO ^c	desorbs and/or converts completely at 100 °C converts almost completely into MSO at 100 °C stable to 100 °C but is largely destabilized at 200 °C, leading to formation of acetate species at 200–400 °C
K-SiAl	protonated and/or H-bonded MSO coordinated Ac ^b coordinated MSO ^c	desorbs and/or converts completely at 100 °C (not examined) (not examined)
Py-SiAl	H-bonded Ac ^a	desorbs almost completely at 100 °C

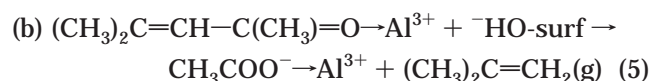
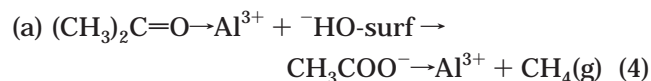
^a (CH₃)₂C=O...^{δ+}HO-Si, νC=O at 1708 cm⁻¹; (CH₃)₂C=O...(^{δ+}HO-Si)₂, νC=O at 1699 cm⁻¹. ^b (CH₃)₂C=O→Al³⁺, involving cu-Al³⁺ sites. ^c (CH₃)₂C=CH-(CH₃)C=O→Al³⁺, involving both π and carbonyl electrons.¹⁷

that makes them more reactive in the addition reaction than surfaces (e.g., of α-Fe₂O₃) on which enolate species were detectable.¹⁹

The importance of Lewis acid sites (□-Al³⁺) for the reaction (eq 1) may be emphasized by the fact that Ac adsorbed on Si and Py-covered SiAl does convert into MSO at RT. The required base catalysis can be provided equally by coordinatively unsaturated oxide sites (O²⁻-surf) or type-I Al-OH groups (terminal OH's), which have been found previously³² to be rather basic in character relative to coexisting type-II (bridging OH's) and -III (multicentered) Al-OH groups. The hydroxylated nature of surfaces of both Al and SiAl may make availability of coordinatively unsaturated oxide sites less likely.

The *addition reaction* is implied by the mechanism established for aldol (self) condensation of acetone in the liquid phase,⁶ since present results can provide no sign of formation of DAA (eq 2). The detection of MSO surface species in Ac/K-SiAl at RT, in which acidic OH's of SiAl are largely replaced by OK groups, may mean that the necessary Bronsted acid sites (⁺H₂O-surf) are those generated in the initial keto-enol conversion (eq 1). The suggested acid-catalyzed *dehydration reaction* of DAA (to form MSO) conforms with frequently reported mechanisms for catalytic dehydration of secondary alcohols on metal oxides.^{30,31} Aluminas are known to be highly selective dehydration catalysts for alcohols.¹⁰

High-temperature conversion of adsorbed MSO into surface acetate species is a common behavior of adsorbed organic oxygenates (alcohols, aldehydes, ketones, and so forth).¹⁰ On surfaces exposing strong acid-base sites, such as the present surfaces of Al and SiAl, acetates are obtained by nucleophilic attack of OH groups on the electrophilic carbonyl carbon of chemisorbed carbonyl compounds.¹⁰ The surface reaction involved may be visualized by the following equations:



The fact that CH₄ and C₃H₇ were detected in the released gas at 300–400 °C may suggest that isobutene was involved in further surface reactions, leading to its decomposition into these two materials.

It is worth noting that SiAl surfaces are far more active catalyst for the above surface reactions of Ac than surfaces of Al. This can be realized from the data summarized in Table 5. The fact that SiAl surfaces expose more obviously Py-detectable Bronsted acidity than Al surfaces may, in terms of the above suggested surface reactions, be the reason behind the extra activity.

Conclusions

The above presented and discussed results may lead to the following conclusions:

(1) Acetone vapor is weakly adsorbed on silica (Table 1), resulting in formation of two differently H-bonded species: (i) an acetone molecule bound to a single terminal Si-OH^{δ+} and (ii) an acetone molecule bound simultaneously to two Si-OH^{δ+} groups. These surface species are desorbed completely at 100 °C, leaving behind neither residual nor conversion species.

(2) On alumina (Table 1), acetone molecules are adsorbed via coordination to Lewis acid sites (coordinatively unsaturated Al³⁺) and via bonding to H-bond donor sites (Al-OH^{δ+}) at RT. Catalyzed by basic Al-OH groups, coordinated acetone is subsequently involved in an aldol-condensation type of surface reaction to yield mesityl oxide surface species. Possible surface intermediates are enolate (or carbanion) and diacetone alcohol species.

(3) On silica-alumina (Table 1), acetone is involved in similar surface adsorptive and consequent reactions to those occurring on alumina at RT. The prominent difference is that on silica-alumina the consequent reactions occur at a faster pace. The higher Bronsted acidity of silica-alumina surfaces is a suggested promoter.

(4) At higher temperatures, adsorbed acetone is converted completely into mesityl oxide at 100 °C (on silica-alumina) and 200 °C (on alumina), and the product species are converted into acetate species at 200–400 °C (on silica-alumina) and 300–400 °C (on alumina). A nucleophilic attack by basic Al-OH groups on the carbonyl carbon of coordinated mesityl oxide is suggested to lead to the generation of surface acetates and releasing of gaseous species.

Acknowledgment. We acknowledge with appreciation Kuwait University Research Administration Grant No. SC 095 and excellent technical assistance found at SAF general facilities (SLC063 & SLD062) of Faculty of Science.